

Neutron Powder Diffraction Study of the Debye–Waller Factor in Nickel using the Reverse Fourier Time-of-Flight Method

BY K. J. TILLI, A. TIITTA AND H. PÖYRY

Reactor Laboratory, Technical Research Centre of Finland, SF-02150 Espoo 15, Finland

(Received 23 July 1979; accepted 1 October 1979)

Abstract

A high-resolution neutron diffraction investigation of a nickel powder sample at room temperature was performed at three different experimental geometries using the ASTACUS diffractometer at Otaniemi. In spite of the correlation between adjacent channels, the diffraction patterns were analysed by the ordinary profile-refinement procedure adapted especially to the present conditions. The correctness of the results was supported by an analysis of the integrated intensities. The weighted mean value for the Debye–Waller parameter, B_{Ni} , of $0.425 (\pm 0.065) \text{ \AA}^2$ was in reasonable agreement with literature values.

1. Introduction

The neutron powder diffraction method has in recent years developed into a powerful experimental tool for the structure analysis of crystalline substances. Behind this progress (for a review, see Cheetham & Taylor, 1977) lies mainly the wide-spread use of the profile-refinement technique, originally introduced by Rietveld (1969), together with the high instrumental resolution attainable today on a number of conventional neutron diffractometers. However, owing to the inevitably poor neutron economy inherent in monochromatic-beam diffractometry, there has been a continuing interest in the development of new methods which permit a significantly better utilization of the available neutron sources. Such efforts have resulted in a variety of white-beam diffraction techniques which have been applied successfully to several recent structure investigations of both single crystals and powders (Hubbard, Quicksall & Jacobson, 1972; Windsor & Sinclair, 1976; Worlton, Jorgensen, Beyerlein & Decker, 1976; Roult & Buévoz, 1977; Balagurov, Borca, Dlouha, Gheorghiu, Mironova & Zlokazov, 1979).

Most of the white-beam diffractometers designed to date are based on the time-of-flight principle, which lends itself immediately to pulsed neutron sources but can also be applied efficiently to steady-state reactors if, instead of a standard Fermi-type chopper, one

employs a pseudorandom or Fourier-type chopper for incident-beam modulation. In particular, the Fourier time-of-flight method not only provides a high duty ratio for beam transmission but it also permits the use of a large beam cross section not limited by the time resolution desired. This technique can thus offer the good resolution required for accurate powder experiments. The application of the Fourier time-of-flight method is quite straightforward in practice, if use is made of the new on-line correlation technique recently developed by Pöyry, Hiismäki & Virjo (1975).

In spite of the several advantages of time-of-flight diffractometry, there have been only very few impressive experimental results so far. One reason for this is the need to take carefully into consideration the wavelength dependence of the inherent factors, such as the incident neutron spectrum, beam attenuation in air and in the sample, extinction and thermal diffuse scattering. Although many authors (Buras, 1969; Hubbard, Quicksall & Jacobson, 1972; Windsor & Sinclair, 1976; Roult & Buévoz, 1977; Balagurov *et al.*, 1979) have discussed how to include these factors in the data analysis, there is still no generally satisfactory recipe available for the problem. Moreover, as for the otherwise efficient correlation time-of-flight methods, there is an additional difficulty in that the experimental data are not statistically independent, which may lead to unexpected errors in the results, unless proper care is given to the correlation between neighbouring channels of the time-of-flight spectra.

In the present paper, the results of the first experiment carried out with the new Fourier time-of-flight diffractometer ASTACUS (Tiitta & Hiismäki, 1979) are presented. The aim of the measurements was to obtain information about the Debye–Waller factor of nickel. The thermal parameter of Ni has been studied by several authors using both X-ray diffraction (Inkinen & Suortti, 1964; Paakkari, 1974) and neutron diffraction (Cooper & Taylor, 1969; Windsor & Sinclair, 1976), but the results are only in very rough agreement. Another objective of this work was to disclose the most important sources of error inherent in a time-of-flight diffraction experiment and, in par-

tical, to shed light on the possible complications arising from the correlations present in spectra measured with the Fourier time-of-flight technique.

2. Experimental

The experiments were carried out by means of the new time-of-flight diffractometer ASTACUS (Tiitta & Hiismäki, 1979) at the 250 kW Triga Mk II reactor of the Technical Research Centre of Finland. The neutron spectra were measured using the reverse time-of-flight method with a Fourier chopper. The maximum modulation frequency of the chopper was 120 kHz leading to a time resolution half-width of about 10 μ s. The measurements were performed in the time-focusing geometry (Hiismäki, Junttila & Piirto, 1975), which permits the use of a large beam area (\varnothing 70 mm) together with a relatively large NE912 glass scintillation detector (2 mm \times \varnothing 190 mm) without worsening the resolution.

The high-purity nickel powder, supplied by Fluka AG, was loosely packed into a flat aluminium container with the inner dimensions 4 \times 80 \times 120 mm. The scattering probability of the sample was 25%.

The scattering experiments were performed at room temperature using three different geometries, as described in Table 1.

Table 1. *Experimental details for Ni powder measurements*

	Experiment		
	A	B	C
Scattering angle ($^\circ$)	135.0	133.5	111.3
Flight path (m)	7.700	5.842	5.998
Measuring time (h)	60	62	102
Number of observed neutrons ($\times 10^7$)	6.378	5.337	17.229
($\sin \theta$)/ λ range (\AA^{-1})	0.40–1.20	0.39–1.18	0.39–1.09
hkl range	220–822	220–644	220–553
Number of independent reflections	23	22	19

3. Method of analysis

The integrated intensities of powder reflections measured on a time-of-flight diffractometer are given by (Buras & Holas, 1968)

$$I_{hkl} = k\lambda^4 \Phi(\lambda) A_s(\lambda) j_{hkl} |F_{hkl}|^2, \quad (1)$$

where k is a scale factor, $\Phi(\lambda)$ the incident neutron spectrum at wavelength λ , $A_s(\lambda)$ the absorption factor for the sample, j_{hkl} the multiplicity factor and F_{hkl} the structure factor of the plane (hkl).

3.1. Incident neutron spectrum

In order to obtain reliable results from a time-of-flight experiment we need exact knowledge of the

wavelength-dependent factors in equation (1). The neutron spectrum $\Phi(\lambda)$ used in the present study has been determined by Tiitta & Hiismäki (1979).

The shape of the incident flux was investigated by fitting a modified Maxwellian distribution, as described by Balagurov *et al.* (1979), to the spectrum. The analysis indicated convincingly that the flux deviates significantly from a Maxwellian, partially because of the strong cut-offs which could not be properly described by using the total cross section of Al powder. The same problem was recognized also by Wilson & Cooper (1973), whereas, on the contrary, both Hubbard, Quicksall & Jacobson (1972) and Balagurov *et al.* (1979) found the incident flux to correspond to a Maxwellian distribution. Evidently, the conclusions are not to be compared with each other on account of the different neutron sources and the dissimilar experimental conditions. Nevertheless, we believe that the use of a theoretical Maxwellian and especially the refinement of its parameters (Hubbard, Quicksall & Jacobson, 1972; Balagurov *et al.*, 1979) is not advisable in connection with an accurate experiment. In addition, in a detailed analysis the errors of the incident spectrum should also be evaluated and properly included in the calculations.

3.2. Sample attenuation

A considerable advantage of powders is that there are no serious extinction problems present. If we assume, as is generally done, that primary extinction can be neglected, then the extinction effects can be included in the attenuation correction by paying attention not only to absorption and incoherent scattering but also to coherent scattering processes. The linear attenuation coefficient $\mu(\lambda)$ can then be written as

$$\mu(\lambda) = \mu_{\text{inc}} + \frac{\lambda^2}{2V_c^2} \sum'_{hkl} |F_{hkl}|^2 j_{hkl} d_{hkl} + \mu_{\text{coh}} \left[1 - \exp\left(-\frac{B}{2d_{hkl}^2}\right) \right] + \mu_0 \lambda, \quad (2)$$

where V_c is the volume of the unit cell, \sum' sums over all reflections for which the interplanar spacing d_{hkl} is greater than $\lambda/2$, and B is the Debye-Waller parameter. μ_{inc} and μ_0 are, respectively, the linear attenuation coefficients for the incoherent scattering and for the absorption at wavelength $\lambda = 1 \text{ \AA}$. In equation (2) the coherent scattering has been divided into the elastic scattering described by the well known formula (Marshall & Lovesey, 1971) and into the inelastic processes treated within the incoherent approximation, which makes use of the wavelength-independent linear attenuation coefficient, μ_{coh} , evaluated from the single nucleus coherent cross section.

A calculation of the linear attenuation coefficient given by equation (2) demands knowledge of the unknown structure factors. Therefore, a proper treatment of the correction should be carried out consistently by iteration in connection with the final refinement of the structure.

3.3. Profile refinement procedure

The neutron powder diffraction data were analysed by the profile-refinement method using the calculated profile at time-of-flight t given by

$$Y_{\text{calc}}(t) = P_1 + P_2 P_4^{1.5} \lambda^{-P_3} \exp(-P_4/\lambda^2) + P_5 \sum_j \frac{C_j}{H_j^2(2\pi)^{1/2}} \exp\left\{-\frac{1}{2}\left(\frac{t-m_j^c}{H_j^c}\right)^2\right\} + P_6 \sum_i \frac{E_i |F_i|^2}{H_i(2\pi)^{1/2}} \exp\left\{-\frac{1}{2}\left(\frac{t-m}{H_i}\right)^2\right\}, \quad (3)$$

where j and i sum over Bragg reflections of the container and the sample, respectively, and

$$E_i = \lambda_i^4 \Phi(\lambda_i) A_s(\lambda_i) j_{hkl}. \quad (4)$$

The background is described by four parameters ($P_1 \dots P_4$), applying the function defined by Worlton, Jorgensen, Beyerlein & Decker (1976). The peak shapes have been approximated by a Gaussian, although the real profile actually represents a convolution of the resolution function of the Fourier method (Pöyry, 1978) with a Gaussian distribution describing the other contributions to the resolution. The peak widths, H_i , can be described by a two-parameter function determined by

$$H_i^2 = P_7 + P_8 m_i^2. \quad (5)$$

m_i is the peak position for the plane (hkl) and is readily calculated in terms of Planck's constant h and neutron mass m by

$$m_i = P_9 + (2mL \sin \theta/h) P_{10} (h^2 + k^2 + l^2)^{-1/2}, \quad (6)$$

where L is the path length and 2θ denotes the scattering angle. The peak positions of the container, m_j^c , were calculated from the well known ratio of the lattice parameters and were, therefore, constrained to the parameter P_{10} .

The integrated intensities C_j of the container reflections were evaluated from the theoretical expressions for aluminium powder. The structure factors F_{hkl} of nickel powder are given by

$$F_{hkl} = 4b_{\text{Ni}} \exp[-P_{11}/(4d_{hkl}^2)], \quad (7)$$

where b_{Ni} is the scattering length of Ni, and P_{11} is the Debye-Waller parameter (B_{Ni}).

The quantity to be minimized in the least-squares refinement with N variables is

$$S^2 = \frac{1}{M-N} \sum_i [Y_{\text{obs}}(t_i) - Y_{\text{calc}}(t_i)]^2 / \sigma_i^2, \quad (8)$$

where M is the number of observations $Y_{\text{obs}}(t_i)$. For uncorrelated data the expression S^2 estimates the variance of an observation of unit weight and should be distributed as $\chi^2/(M-N)$ with $M-N$ degrees of freedom. For a satisfactory theoretical model S^2 should, therefore, have a value close to unity if the weights σ_i are correct.

Unfortunately, the above considerations do not apply to the present case because of the correlation between the observations. In a proper refinement we should therefore use the well known equations for correlated data (Draper & Smith, 1966) and, in addition, define anew the quantity S^2 . The essential increment of the revised analysis is the inclusion of the variance-covariance matrix for observations. In the present case, this matrix is of the order of 1500×1500 and it is difficult to obtain detailed information on its form, although in the first approximation it can be evaluated from the equations given by Pöyry, Hiismäki & Virjo (1975). For these reasons it is uncertain whether the correct analysis with the inversion of the variance-covariance matrix can be performed with success. Therefore, in the present context the correlation was neglected, and the standard least-squares method for uncorrelated observations was applied. Fortunately, the estimates obtained in this way are still unbiased but they do not have the minimum variance (Draper & Smith, 1966). Furthermore, great care should be taken when the evaluated variances of the refined parameters are examined and when significance tests are performed using methods originally designed for uncorrelated observations. Besides, the expected value of S^2 obtained from equation (8) is then not known. But it can be shown that for a simple background experiment analysed with the one-parameter function $Y_{\text{calc}} = P_1$ the expected value is still unity.

The quantity often used in the profile analysis to measure the quality of fit is the R_{profile} factor defined by Rietveld (1969). However, its application to correlation methods is inconvenient because of the difficulties in obtaining reliable estimates for absolute values of the neutron spectrum (Pöyry, Hiismäki & Virjo, 1975). In addition, the R_{profile} factors quoted in connection with correlation methods are not to be compared to the values obtained with conventional diffractometers on account of the quite different origin of the experimental variances. Consequently, in the present context the quality of fit is evaluated only by means of the quantity S^2 .

In a proper analysis the observations in equation (8) should be correctly weighted by taking into account all random and systematic errors in the measurement. The

variances σ_i^2 can be written as

$$\sigma_i^2 = \sigma_{\text{exp}}^2(t_i) + Y_{\text{peak}}^2(t_i)\sigma_E^2/E_{hkl}^2, \quad (9)$$

where σ_{exp}^2 is obtained from the counting statistics of the experiment and is for correlation methods directly proportional to the total number of observed neutrons. $Y_{\text{peak}}(t_i)$ is the calculated peak intensity at time-of-flight t_i . The variance σ_E^2 arises from errors in E_{hkl} and is readily calculated by

$$\frac{\sigma_E^2}{E_{hkl}^2} = \left[4 + \frac{\lambda}{\Phi} \frac{\partial \Phi}{\partial \lambda} \right]^2 \sigma_\theta^2 \cot^2 \theta + \frac{\sigma_\Phi^2}{\Phi^2}. \quad (10)$$

The former term describes the errors arising from Bragg angle determination with the estimated standard deviation σ_θ . The latter term includes all inaccuracies inherent in the incident neutron spectrum estimate, where the most significant errors are due to uncertain corrections.

The fitting based on the above considerations was performed on the full-matrix least-squares profile-refinement program *PRPNUCL* written for the CDC Cyber 170 computer having 32 K words core storage available for the users. The attenuation corrections were evaluated using initial values for the parameters before the minimization. When required, the program can, in addition to the parameters mentioned above, refine also the occupation numbers, fractional coordinates and anisotropic temperature factors. Moreover, there is the possibility of introducing linear constraints between all parameters.

4. Results of the profile analysis

Fig. 1 presents the observed neutron diffraction patterns for the nickel powder sample. The refined parameters are given in Table 2 together with the agreement factors.

The quality of fit can be estimated by calculating the confidence interval of $100(1 - 2\alpha)$ per cent (Abrahams, 1969)

$$U_\alpha = [S^2/(S^2)_\alpha]^{1/2}, \dots, [S^2/(S^2)_{1-\alpha}]^{1/2}, \quad (11)$$

where $(S^2)_\alpha = \chi_\alpha^2/(M - N)$, and by investigating whether the calculated range includes unity. Examination of the intervals in Table 2 shows, at the significance level of 0.1%, that the values obtained for S^2 are too large. However, because of the correlation we cannot, on using the above considerations based on the tests suitable only for uncorrelated observations, conclude either the theoretical model or the variances in equation (8) to be incorrect.

Additional insight into the quality of fit can be obtained by examining the difference profiles depicted in Fig. 1. The agreement between the observed and calculated profiles is good over the range of measurements, showing no difficulties in fitting the peak

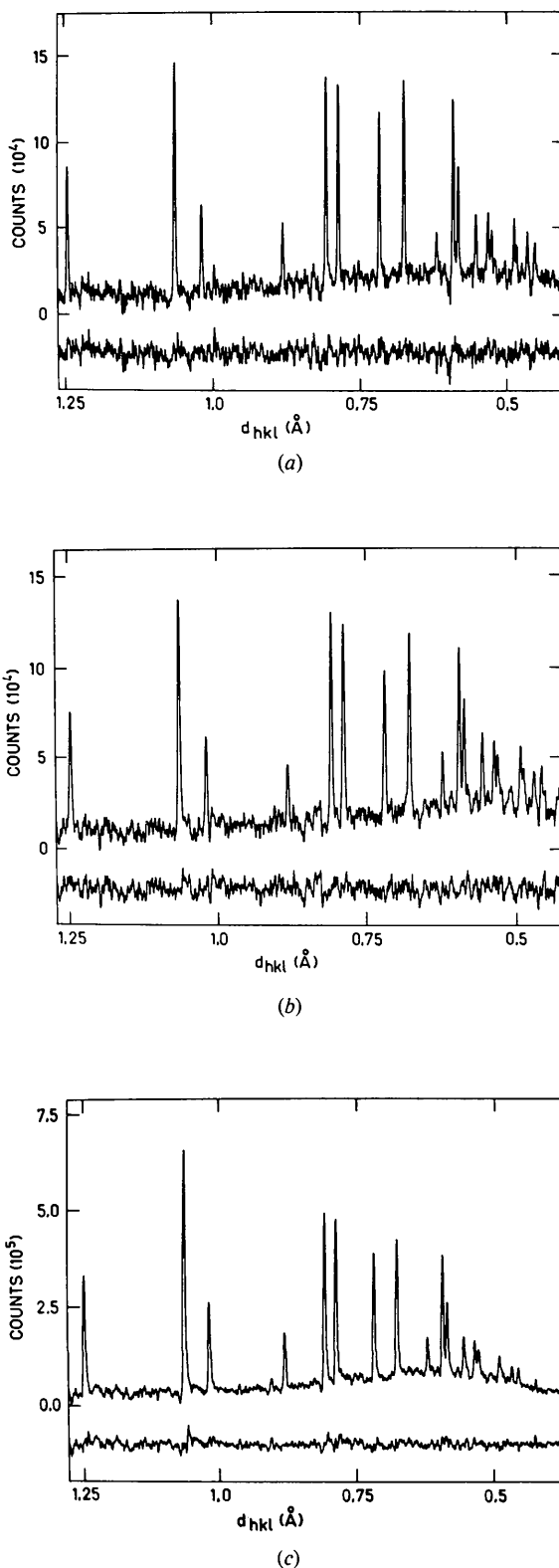


Fig. 1. The observed neutron diffraction patterns for nickel powder. The differences between the experimental and calculated profiles are also shown.

intensities. Therefore, the values of S^2 , at least those obtained from measurements *A* and *B*, are acceptable. The quantity S^2 reflects the quality of the whole fit and is, thus, strongly affected by the inaccuracies in the assumed shape of the background. In particular, the large value of S^2 in measurement *C* implies, in view of the good statistical accuracy, that such errors are present in the background. This conclusion was also confirmed by the usual analysis-of-variance techniques.

The incoherent background generally reflects the shape of the incident neutron spectrum, which, as mentioned above, deviates significantly from the Maxwellian. However, the statistical accuracies of the present experiments are inadequate to disclose this deviation, which is due to the inherent difficulty of correlation methods to obtain reliable estimates for flat regions of the spectra. In a refinement the last-mentioned feature becomes visible in the large standard deviations of the background parameters and in the considerable correlation coefficient ($\sim 10\%$) between the intensity parameters.

A more important effect than that mentioned above is due to the errors in the low-frequency operation of the neutron chopper giving rise to a resolution function with a peak superimposed on a small but broad negative component (Pöyry, 1978). A similar but positive distortion is perhaps caused by multiple

scattering and thermal diffuse scattering. The broad humps arising from these effects can partly be described by the function given in equation (3), especially if the peaks are close enough, whereas otherwise the refined parameters contain systematic errors of unpredictable magnitude. The spectra shown in Fig. 1 do not, however, display such broad distortions so that the extent of the bias in the estimates is presumably small as compared with the overall accuracy.

The value of S^2 depends also on the assignment of weights $1/\sigma_i^2$ in equation (8). The variances σ_i^2 contain two terms arising from the counting statistics and from the incident spectrum inaccuracy. The importance of the latter depends on the accuracy of the measurement. In the present work, the two sources of error represented in equation (9) are of the same order of magnitude only in the largest peaks. Therefore, the inclusion of the variance arising from the incident spectrum inaccuracy did not improve the fits significantly. However, it is clear that the ultimate accuracy obtainable by white-beam techniques is determined entirely by this term, which certainly cannot be ignored when reliable estimates for structural parameters are desired.

The Debye–Waller parameters obtained under the different experimental conditions are consistent with each other. The weighted mean value $\bar{B} = 0.425 (\pm 0.065) \text{ \AA}^2$ is in agreement with the value of $0.426 (\pm 0.009) \text{ \AA}^2$ from the neutron measurement of Cooper & Taylor (1969). Also, the earlier X-ray determinations of $0.37 (\pm 0.02) \text{ \AA}^2$ (Inkinen & Suortti, 1964) and $0.386 (\pm 0.012) \text{ \AA}^2$ (Paakkari, 1974) agree with the mean value, although the difference from the value from experiment *C* is highly significant. However, the present work does not support the result $B = 0.34 (\pm 0.04) \text{ \AA}^2$ measured by Windsor & Sinclair (1976) using time-of-flight neutron diffraction. The anharmonicity of the lattice vibrations observed by Windsor & Sinclair (1976) could not be confirmed by the present work.

In the above analysis we paid no attention to thermal diffuse scattering even if it certainly has an effect upon the value obtained for the Debye–Waller factor. The reason for this omission is that no theoretical treatment of the TDS problem in time-of-flight diffraction is available as yet. Because of the increase in phonon cross section with scattering vector the effect may become important for the high-order reflections. However, the TDS contributions are probably broad on a time-of-flight scale, as Windsor & Sinclair (1976) point out. Moreover, the time-focusing of the ASTACUS diffractometer even enhances the broadness of the inelastic contributions, which thus could partially be taken into consideration by the background. Therefore, in the present case the neglect of the TDS correction presumably leads to less severe

Table 2. *Final refinement parameters and agreement factors for the measurements*

Estimated standard deviations in the last significant digit are given in parentheses.

	<i>A</i>	Experiment <i>B</i>	<i>C</i>
Background			
$P_1 (\times 10^3)$	9.40 (94)	10.46 (42)	33.64 (79)
$P_2 (\times 10^5)$	0.63 (7)	0.79 (14)	7.6 (12)
$P_3 (\text{Å}^2)$	4.94 (54)	7.04 (61)	10.12 (46)
P_4	2.85 (31)	3.44 (33)	5.00 (23)
Container			
P_5	3.53 (90)	2.92 (73)	11.0 (19)
Peak width			
$P_7 (\mu\text{s}^2)$	20.15 (93)	18.9 (10)	16.55 (73)
$P_8 (\times 10^{-6})$	0.25 (9)	0.64 (18)	1.14 (13)
Peak position			
$P_9 (\mu\text{s})$	-0.56 (19)	-0.77 (21)	-1.02 (16)
$P_{10} (\text{Å})^*$	3.52370 (22)	3.52375 (32)	3.52389 (23)
Sample			
P_6	10.58 (20)	7.81 (17)	42.02 (58)
$P_{11} = B_{\text{Ni}} (\text{Å}^2)$	0.412 (20)	0.403 (23)	0.451 (19)
Fit quality			
S^2	1.24	1.19	1.90
$U_{0.001}$	1.06–1.18	1.02–1.17	1.29–1.47

* The lattice parameters are not calibrated.

effects than in conventional fixed-wavelength powder studies.

5. Integrated intensity method

In order to obtain additional insight into the reliability of the results and into the influence of the correlation, the Debye-Waller parameters were also evaluated from the structure factors. For this reason, the program was modified so that the individual structure factors F_i in equation (3) could be refined. The Debye-Waller parameters were then estimated using the ordinary weighted least-squares method for uncorrelated observations (Draper & Smith, 1966). The results of the fitting are depicted in Fig. 2. The parameters and the agreement factors are reported in Table 3 together with the weighted R factors $R_w = 100\{\sum w[F(\text{obs.}) - F(\text{calc.})]^2 / \sum wF^2(\text{obs.})\}^{1/2}$, where the weights $w_i = 1/\sigma_i^2$ are obtained from the variances σ_i^2 of the structure factors.

Examination of the S^2 values and the $U_{0.01}$ ranges in Table 3 shows that either the theoretical model or the weights are incorrect. The least-squares fits depicted in Fig. 2 show, however, no systematic departures from the assumed linearity. Doubts about the invalidity of the theoretical model can, therefore, be restricted to the errors in the incident neutron spectrum determination.

The above considerations can be examined in a detailed way by inquiring into the distribution of the weighted differences $\Delta_i = [F_i(\text{obs.}) - F_i(\text{calc.})]/\sigma_i$. A comparison with the normal distribution by the normal probability plots (*International Tables for X-ray*

Table 3. Results from the integrated intensity method

	Experiment		
	A	B	C
B (\AA^2)	0.410 (30)	0.389 (33)	0.432 (25)
S_F^2	3.72	3.62	3.87
$U_{0.01}$	1.41-3.00	1.38-3.00	1.40-3.20
R_w (%)	2.82	3.00	1.84

Crystallography, 1974) is made in Fig. 3. The assumption of a normal error distribution, which can be tested by looking at the straightness of the lines, is unjustified only in connection with experiment C, which is a new manifestation of the difficulties in the background determination. The slopes of larger than unity indicate that the variances have been uniformly underestimated. The unacceptably small standard deviations are probably due to the omission of the correlation in the profile analysis, this giving rise to a parameter estimation not having minimum variances as well as to erroneous estimates for standard deviations. However, it is impossible to decide from the above arguments which is the reason for the observed underestimation, but intuitively the intensities of the peaks can be expected to have too small e.s.d.'s, owing to the correlation. As a result of the latter the effective number of observations in one peak is less than the number of channels defining the peak.

The Debye-Waller parameters and their estimated standard deviations obtained from the structure factors are of the same size as the results from the profile analysis (Table 2). The small differences can be

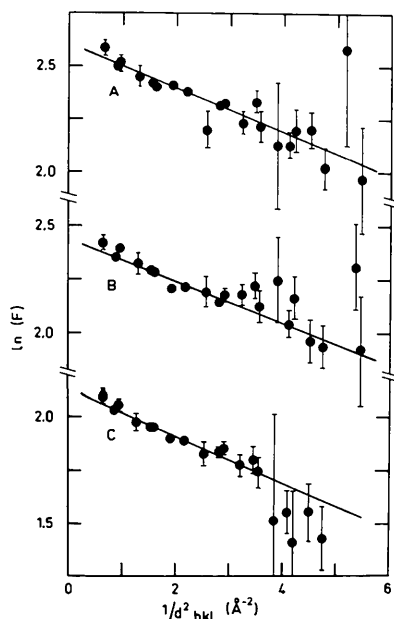


Fig. 2. Plots of $\ln(F)$ as a function of $1/d_{hkl}^2$. The points with the 95% confidence ranges represent data from individual Bragg peaks. The solid lines are the least-squares fits.

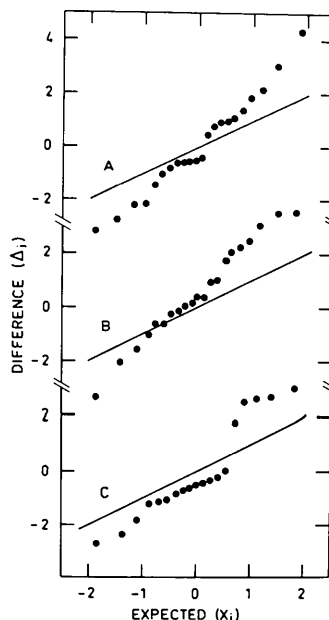


Fig. 3. Normal probability plots of the ranked weighted differences Δ_i between the residuals of the least-squares analysis and the expected values x_i for a normal distribution. The slopes of unity have been indicated by solid lines.

explained by the omission of the slight correlation between the structure factors in the least-squares analysis. The agreement of the estimated standard deviations is of great importance. In the integrated intensity method the e.s.d.'s are evaluated from the least-squares residuals whereby the uniform underestimation of the variances is insignificant. Hence, the variance estimates obtained by the profile-refinement method are reasonable, which can be explained by a diminution of the influence of the correlation when the spectrum comprises a large number of separated peaks.

6. Conclusions

The results of the present paper demonstrate that reverse time-of-flight diffractometers with Fourier choppers offer a useful means for structure analysis. The ultimate accuracy obtainable with this white-beam technique is determined by the precision of the incident neutron flux estimate, which must, therefore, be taken into account in a proper analysis.

The theoretically rigorous method for the refinement of diffraction data measured with the correlation technique was considered impracticable, for which reason the ordinary method was applied yielding unreliable estimates for parameters evaluated from only one reflection. Fortunately, a powder diffraction pattern contains a large number of peaks so that reliable estimates can be obtained for structural parameters, but nevertheless part of the high efficiency of correlation methods will be lost on account of the cautious interpretations.

The authors wish to thank Dr P. Hiismäki for many helpful discussions and Mr H.-E. Karlsson for his valuable assistance with the experiments.

Acta Cryst. (1980). **A36**, 259–265

Statistics of Ion Distribution in 1D and 2D Mixed Crystals

BY CLAUD FRIEBEL

Sonderforschungsbereich 127 (Kristallstruktur und chemische Bindung) und Fachbereich Chemie der Universität Marburg, Lahnberge, D-3550 Marburg, Federal Republic of Germany

(Received 15 May 1979; accepted 2 October 1979)

Abstract

A statistical distribution of ions M in lattices or partial lattices $\infty[A_{1-x}M_xL_m]$ of mixed crystals being assumed, the probability functions $P_j^{(v)}(x)$ for single coordination polyhedra ML_n ($j = 1$), pairs ($j = 2$) and

0567-7394/80/020259-07\$01.00

References

- ABRAHAMS, S. C. (1969). *Acta Cryst.* **A25**, 165–172.
 BALAGUROV, A. M., BORCA, E., DLOUHA, M., GHEORGHIU, Z., MIRONOVA, G. M. & ZLOKAZOV, V. B. (1979). *Acta Cryst.* **A35**, 131–136.
 BURAS, B. (1969). Report INR 1108/II/PS. Institute of Nuclear Research, Warszawa.
 BURAS, B. & HOLAS, A. (1968). *Nukleonika*, **13**, 591–619.
 CHEETHAM, A. K. & TAYLOR, J. C. (1977). *J. Solid State Chem.* **21**, 253–275.
 COOPER, M. J. & TAYLOR, R. I. (1969). *Acta Cryst.* **A25**, 714–715.
 DRAPER, N. R. & SMITH, H. (1966). *Applied Regression Analysis*, pp. 77–81. New York: John Wiley.
 HIISMÄKI, P., JUNTILA, J. & PIIRTO, A. (1975). *Nucl. Instrum. Methods*, **126**, 435–443.
 HUBBARD, C. R., QUICKSALL, C. O. & JACOBSON, R. A. (1972). *Acta Cryst.* **A28**, 236–245.
 INKINEN, O. & SUORTTI, P. (1964). *Ann. Acad. Sci. Fenn. Ser. A6*, p. 147.
International Tables for X-ray Crystallography (1974). Vol. IV. Birmingham: Kynoch Press.
 MARSHALL, W. & LOVESEY, S. W. (1971). *Theory of Thermal Neutron Scattering*, p. 35. Oxford Univ. Press.
 PAAKKARI, T. (1974). *Acta Cryst.* **A30**, 83–86.
 PÖYRY, H. (1978). *Nucl. Instrum. Methods*, **156**, 499–514.
 PÖYRY, H., HIISMÄKI, P. & VIRJO, A. (1975). *Nucl. Instrum. Methods*, **126**, 421–433.
 RIETVELD, H. M. (1969). *J. Appl. Cryst.* **2**, 65–71.
 ROULT, G. & BUÉVOZ, J. L. (1977). *Rev. Phys. Appl.* **12**, 581–590.
 TIITTA, A. & HIISMÄKI, P. (1979). *Nucl. Instrum. Methods*, **163**, 427–436.
 WILSON, S. A. & COOPER, M. J. (1973). *Acta Cryst.* **A29**, 90–91.
 WINDSOR, C. G. & SINCLAIR, R. N. (1976). *Acta Cryst.* **A32**, 395–409.
 WORLTON, T. G., JORGENSEN, J. D., BEYERLEIN, R. A. & DECKER, D. L. (1976). *Nucl. Instrum. Methods*, **137**, 331–337.

larger clusters of ML_n groups ($j > 2$) in 1D ($v = 2$) and v -connected 2D systems ($v = 3, 4, 6$) are calculated. On raising the connecting number v , increasing cluster probabilities are distinctly shifted to lower concentrations x of the foreign ion M . For a relation between the numerical values $P(x)$ and experimental results, the

© 1980 International Union of Crystallography